In Vitro Cell. Dev. Biol.—Animal 35:403–409, July–August 1999

1071-2690/99 $05.00+0.00

A NEW HUMAN PROSTATE CARCINOMA CELL LINE, 22R*v1*

R. MICHAEL SRAMKOSKI, THOMAS G. PRETLOW II, JOSEPH M. GIACONIA, THERESA P. PRETLOW, STUART SCHWARTZ, MAN-SUN SY, SUSAN R. MARENGO, JOHNG S. RHIM, DESHENG ZHANG, AND JAMES W. JACOBBERGER[1]

Cancer Research Center (R. M. S., T. G. P, T. P. P., S. S., M.-S. S., S. R. M., D. Z., J. W. J.), Departments of Genetics (S. S., J. W. J.), Pathology (T. G. P., J. M. G., T. P. P., M.-S. S.), and Urology (S. R. M.), Case Western Reserve University, Cleveland, Ohio 44106, and Laboratory of Biochemical Physiology, National Cancer Institute (J. S. R.), Frederick, Maryland 21702

(Received 27 October 1998; accepted 19 February 1999)

SUMMARY

A cell line has been derived from a human prostatic carcinoma xenograft, CWR22R. This represents one of very few available cell lines representative of this disease. The cell line is derived from a xenograft that was serially propagated in mice after castration-induced regression and relapse of the parental, androgen-dependent CWR22 xenograft. Flow cytometric and cytogenetic analysis showed that this cell line represents one hyper DNA-diploid stem line with two clonal, evolved cytogenetic sublines. The basic karyotype is close to that of the grandparent xenograft, CWR22, and is relatively simple with 50 chromosomes. In nude mice, the line forms tumors with morphology similar to that of the xenografts, and like the parental CWR22 and CWR22R xenografts, this cell line expresses prostate specific antigen. Growth is weakly stimulated by dihydroxytestosterone and lysates are immunoreactive with androgen receptor antibody by Western blot analysis. Growth is stimulated by epidermal growth factor but is not inhibited by transforming growth factor-β1.

Key words: cancer; epithelial cell; xenograft; androgen response; cell growth; EGF; TGF-β.

INTRODUCTION

A xenograft model for primary human prostate carcinoma has been previously established and described (4,23,28,37). This model has some interesting characteristics. Chief among these is that the CWR22 xenograft forms androgen-dependent tumors that secrete prostate specific antigen (PSA) into the blood stream of mice at levels related to tumor burden (37), regresses after castration, and relapses 3–10 mo. after androgen ablation (23). Relapsed tumors, designated CWR22R, have been serially transplanted (23). One limitation of the model is that to our knowledge, cell lines have not been established from the xenografts. In vitro, we have had difficulty with mouse stromal cell growth that ultimately limited the growth of the human cells and dominated the culture. We now report that we have established one strain of CWR22R (2152) as a permanent cell line. To circumvent past problems with overgrowth of mouse stromal cells, we used a combination of serial fluorescence-activated cell sorting of tumor cells expressing human CD44 (24), and subculture on irradiated mouse fibroblast feeder layers. CD44 cell sorting was used to reduce the mouse cell population, and feeder layers were used to assist tumor cell attachment and human epithelial cell growth.

The resultant cell line, 22R*v1*, produces tumors in nude mice with a morphology similar to that of the parental xenograft and secretes PSA. The cell line shows one hyper-diploid stem line by DNA flow cytometry and one main stem line by karyotype analysis with 50 chromosomes. The karyotype of the cell line is similar to that of the CWR22 xenograft. 22R*v1* showed a response to dihydroxytestosterone (DHT) and epidermal growth factor (EGF) but abnormally to transforming growth factor beta 1 (TGF-β1). Androgen receptors were detected immunologically.

MATERIALS AND METHODS

Xenografts. CWR22R tumors were serially transplanted as previously described (23). Nude mice, 4–8 wk old, from the CWRU Cancer Center Athymic Core Facility were housed singly and fed ad libitum. Cells were prepared from tumors by digestion with Pronase (23,37), washed with RPMI 1640 (GIBCO BRL, Gaithersburg, MD) with 20% calf serum (GIBCO), filtered through a single layer of 250-μm-pore Nitex (Tetko, Inc., Briarcliff Manor, NY), and counted with a hemacytometer. Cells were frozen over liquid N_2 in medium with 8% dimethyl sulfoxide and 20% calf serum. Mice were injected with either fresh or frozen cells suspended in Matrigel (27) after being thawed and washed with serum-containing medium. The cell line 22R*v1* was injected into nude mice in a similar manner.

Cell culture. Dissociated tumors were kept on ice until plating onto irradiated STO cell (ATCC, Rockville, MD) feeder layers at 1–2 × 10^6 cells per 10-cm plate (Corning Glass Works, Corning, NY). Feeder layers were prepared in advance from exponentially growing STO cell cultures. Cells were trypsinized as described and irradiated in suspension with a ^{60}Co source (50 Gy). In all, 3 × 10^6 irradiated cells were plated per 10-cm dish. Cultures were fed with RPMI 1640 with 10% fetal bovine serum (FBS) (Sigma Chemical Co., St. Louis, MO). Cells from the CWR22R xenograft were later grown on 10-cm dishes from which the STO feeders were removed by scraping, and the cell line, 22R*v1*, derived from the CWR22R xenograft was serially cultured on plastic tissue culture dishes without feeder layers or other treatment. DU 145 (21) and PC-3 (16) cells were grown on plastic plates in Dulbecco's modified Eagle's medium (DMEM) with 5% FBS and 5% calf serum (Sigma). LNCaP cells were grown in T medium as described (9). MLC cells [designated as pRNS-1-1 (18)], originally established by transfecting primary normal human adult prostatic cells with an origin-defective SV40 genome, retain prostate epithelial morphology and cytokeratin expression profile and are nontumorigenic in nude mice. MLC cells were cultured in T medium.

[1]To whom correspondence should be addressed at Case Western Reserve University, Cancer Research Center, 10900 Euclid Avenue, Cleveland, Ohio 44106-4944.

Western blot analysis. Immunoprecipitation was performed as described (10). All steps were performed at 4° C with agitation. Briefly, confluent cell cultures were lysed in radioimmunoprecipitation assay (RIPA) supplemented with a protease cocktail (1 m*M* phenylmethylsulfonyl fluoride, 2 mg pepstatin per ml, 0.2 U aprotinin per ml, and 0.5 mg leupeptin per ml). Two milligrams of protein were precleared with 10% vol/vol of bovine serum albumin (BSA)-blocked Protein A-Sepharose beads (Bio-Rad Laboratories, Hercules, CA) and exposed to rabbit anti-androgen receptor polyclonal antibody (Santa Cruz Biotechnology, Inc., Santa Cruz, CA). Protein A agarose beads were used to capture antigen-antibody complexes and were washed with RIPA. One-half of the capture beads were subjected to 6% sodium dodecyl sulfate-polyacrylamide gel electrophoresis under reducing conditions, electroblotted to polyvinylidine difluoride membrane (0.2 mm, Bio-Rad) and subjected to immunoblot analysis as previously described (19). Androgen receptor antibodies were used at a dilution of 1:1500, and secondary, horseradish peroxidase-conjugated donkey anti-rabbit antibodies (Amersham, Arlington Heights, IL) at a dilution of 1:2000. Antigen-antibody complexes were detected with an enhanced chemiluminescence kit (Amersham).

Growth factor response. 22R*v1* cells were plated at 3.1×10^5 per 6-cm dish in Phenol Red-free DMEM with 10% FBS. Twenty-four h later, the medium was removed; the cells were washed twice with phosphate-buffered saline (150 m*M* NaCl, 10 m*M* sodium phosphate, pH 7.2) (PBS), and DMEM with 1% BSA (Sigma) without additives other than the following. Final concentrations of additives were EGF (U.S. Biochemicals, Cleveland, OH) at 100 ng/ml, DHT (Sigma) at 10^{-10} or 10^{-8} *M*, TGF-β1 (Sigma) at 10 ng/ml. Control cells did not receive growth factors. At 3 and 6 d after factor addition, cells were trypsinized and counted with an electrical resistance counter (Coulter Electronics, Inc., Hialeah, FL). On Day 3, cultures were refed with the same medium and additives.

Immunochemical staining, flow cytometry, and cell sorting. Cultures were dissociated with trypsin-EDTA (29), washed twice with PBS, once with PBS with 2% FBS, then stained for 30 min on ice with a previously described monoclonal antibody, A3, specific for CD44 (12) followed with fluorescein isothiocyanate conjugated goat anti-mouse Fab'2 (CalTag, South San Francisco, CA). Stained cells were kept on ice until sorting. The cells were analyzed and sorted with an Elite flow cytometer/cell sorter (Coulter) with forward and right angle light scatter as primary gates. Cytokeratin expression was measured after staining methanol-fixed cells as described (29) with a monoclonal antibody against 45–56 kDa human cytokeratins (DAKO, cat # M0821, Carpinteria, CA) and a CY5™-conjugated goat anti-mouse antibody (CalTag) and counterstaining with Hoechst 33342 (HO) (Calbiochem-Novabiochem, San Diego, CA) to detect DNA content. To determine the DNA index, prostate cell lines and blood mononuclear cells were trypsinized, permeabilized with 0.1% Triton X-100 in PBS, and stained with 50 μg propidium diiodide per ml as previously described (29). Data were analyzed with list mode software (WinList, Verity House, Topsham, ME) and some plots were made with Win MDI 2.7 (Joe Trotter, Scripps Research Institute, La Jolla, CA). The percentage of positive cells was determined by gating in two-parameter analyses and by a histogram subtraction method for single parameter analyses (cytokeratin).

Cytogenetic analysis. Proliferating cells were treated with colcemid (0.5 μg/culture) for 30 min, swelled in 0.75 *M* KCl, fixed for 15 min with 3:1 methanol:acetic acid three times. Banded metaphases were prepared by trypsin pretreatment, followed by Giemsa staining to produce G-bands (30). Twenty-one cells were analyzed.

Histology. Tumors were fixed in formalin, embedded in paraffin, sectioned at 5 μm, then stained with hematoxylin and eosin.

Results and Discussion

Cell sorting. Our early experiments aimed at culturing the xenograft lines ended with cultures that were overgrown with mouse cells (J. W. J., unpublished). Therefore, we attempted to reduce the number of mouse cells by culturing surgically resected, dispersed xenografts on irradiated STO feeder cells to promote robust epithelial growth and potentially inhibit mouse cell growth. Epithelial colonies were visible by phase-contrast microscopy by 7 d after plating (Fig. 1 *A*). Mouse stromal cell growth was present also (e.g., Fig. 1 *C*, *arrow*). At that time, cultures were trypsinized and stained for human CD44 in an indirect immunofluorescent assay. DU 145 and LNCaP

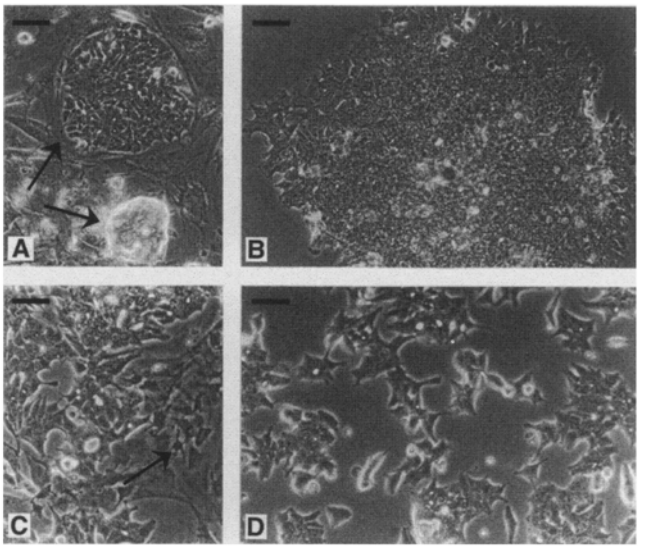

FIG. 1. Cultured CWR22R and 22R*v1* cells. *A*, 22R*v1* on feeder layer at 7 d. *Arrows* point to colonies at various stages of implantation into the feeder layer. The upper colony has implanted and spread; the lower, refractile colony has not. Eventually most colonies embed. *B*, Typical colony of 22R*v1* after 14 d on feeder layers. By this time, most of the feeder layer is gone unless replenished. The colonies in *A* and *B* are directly comparable in size and typical for Days 7 and 14. *C*, 22R*v1* cells were injected into a nude mouse. After tumor formation, the xenograft was cultured on plastic. *Arrow* points to mouse stromal cells. *D*, 22R*v1* cells growing on plastic. *A* and *B: bars*, 90 μm; *C* and *D*: *bars*, 63 μm.

prostate cancer cell lines were used to verify CD44 staining. DU 145 cells strongly express immunoreactive surface CD44, and LNCaP cells do not (32). DU 145 cells were 14 times more fluorescent than LNCaP cells, and 96% were positive relative to the LNCaP control.

Typical results for a cell sorting experiment of xenograft cultures are shown in Fig. 2. The top panel in the figure is an initial sorting analysis. The data show that a significant number of the mouse cells in the culture bound IgG specifically. Compare the sample stained with Fab'2 to that stained with nonspecific IgG2a [the population marked by an arrow when stained and delimited by a dashed oval when unstained represent Fc-binding cells]. Analysis of CD44-stained samples (Fig. 2, *Column C*) showed that the CWR22R human tumor xenograft cells displayed intermediate levels of fluorescence compared to the major population of the isotype control sample, the Fc-binding cells (Column B), or DU 145 cells (not shown). Therefore, we constrained the sorting gate to the center of the CD44 specific distribution in an attempt to exclude most Fc-binding cells and most CD44-negative cells from the major population not binding Fc. The histogram in the top panel (Column D) shows the fluorescence of the sorted population. The lower panel in Fig. 2 shows similar data for the sorted cells after 17 d of growth on feeder layers. Column B shows that IgG-binding cells are still present, but that the culture is now enriched for human cells that express CD44. The enrichment is approximately twofold. Since we did not maintain parallel unsorted cultures, we cannot be certain that a cell sorting step is required for successful isolation of this cell line; however, all attempts to derive a line from CWR22R xenografts by subpassage alone have failed due to overgrowth of fibroblast-like cells, even when the fraction of epithelial cells in the initial plating was very high. The cell line reported

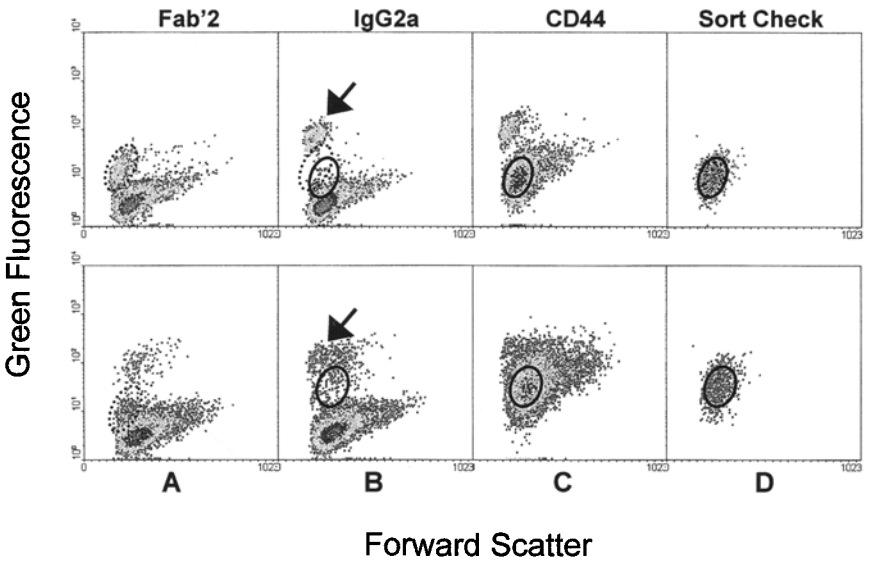

FIG. 2. Cell sorting of cultured CWR22R xenograft cells. *Top Panel*: Cell staining after 14 d of culture on STO feeder cells. *Lower Panel*: Cell staining after cell sorting of CD44-positive cells as depicted in the top panel and reculture on STO feeder cells for 17 d. *Column A* shows cells stained with an FITC-conjugated Fab'2 goat anti-mouse secondary antibody alone. *Column B* shows cells stained with an IgG2a isotype control and the same FITC-Fab'2 secondary. IgG-binding mouse cells are evident in column A (*dotted region*) and column B (*arrow*). *Column C* shows cells reacted with mouse anti-human CD44 antibody, A3, and the same secondary. Sorting gates (continuous region) were set on the basis of the IgG isotype control (*column B*) with the intention to gate between mouse IgG-binding and CD44-unreactive cell populations. Controls for anti-CD44 specificity were LNCaP (CD44 negative) and DU 145 (CD44 positive) (data not shown). CD44-positive cells represented about 37% of the population in the top panel and about 86% of the population in the bottom panel. *Column D* shows an analysis of the sorted cells providing a visualization of sort purity.

here was sorted and recultured on feeder layers three times.

Culture conditions. One problem with STO feeder layers is that it is difficult to determine whether any significant fibroblast contamination remains by microscopic inspection. Therefore, after the cell line appeared to be free of mouse cells, we attempted culture on tissue culture dishes on which irradiated STO cells had been plated and cultured for 2 d, then scraped. The CWR22R xenograft line proved to grow well under these conditions, and after a few passages, we attempted growth on plastic tissue culture dishes without prior treatment. The line also grew well on plastic (Fig. 1 *D* and 3). We do not know whether the intermediary step on scraped plates is necessary. The cell line was named 22R*v1* (v1 = variant 1). The xenograft from which it was derived was obtained in January 1997; the isolation experiments and subsequent regrowth were performed until April; and the first frozen passage was May 8, 1997. The isolated cell line was continuously cultured from May 1997 to December 1998 with approximately weekly passages. At a split ratio of 1/50, the population doubles approximately three times in 7 d (Fig. 5), therefore the cell line underwent approximately 240 population doublings during that time.

Epithelial lineage. 22R*v1* cells were immunoreactive with a monoclonal antibody specific for 45–56 kDa human cytokeratins by flow cytometric analysis (Fig. 3). This analysis showed a unimodal fluorescent population that was 93.8 ± 0.3% positive.

DNA content. Correlated DNA analysis showed that the CWR22R xenograft line has a single stem line (Fig. 3). DNA content analysis showed that 22R*v1* was hyper-diploid with a DNA index of 1.3–1.4 (Table 1). The histogram of this early passage (July 1997) showed no evidence of any other stem line and little evidence of an endoreduplicating subpopulation (low percentage of 2C G_2 + M and infrequent S and G_2 + M phase cells greater than 4C, Fig. 3). Comparison by flow cytometric DNA analysis of an early cryopreserved passage and a lab strain passaged continuously for approximately 18 mo. showed clear evidence for an endoreduplicated population in the late passage and no evidence in the early passage. Evidence consisted of easily identifiable 4C S and G_2 + M phases. For the late passage cells, 27% had a DNA content of 4C or greater compared to 10% 4C G_2 + M cells in the early passage. Late passage cells do not show a significant difference in stem line DNA content (Table 1) or any evidence for more than one stem line. However, we have analyzed 22R*v1* provided to and maintained by another laboratory, and this strain had a very high percentage of 4C cells. Therefore, the evidence we have at present suggests that this cell line can undergo endoreduplication that can result in a stable 4C genotype.

Cytogenetics. In contrast to other reported prostate cancer cell lines, the changes in ploidy and karyotype of 22R*v1* cells appear simpler. The modal chromosome number was 50 (N = 15) with 6 hypermodal cells. The karyotype was 50, XY, +i(1)(q10), der(2)t(2;4)(p13↔1)del(2)(q13q33), der(4)t(2;4)(p13↔1), t(6;14)(q15↔2), +7, +8, +12[13]/51, idem, +3[2]/51, idem, t(1:12)(p11↑3), +3[4]/50, idem, del(1)(p10)[2].

Cytogenetic analysis of the 21 metaphases revealed that the basic stem line was that of the original xenograft, CWR22, with some evolution (37). Additionally, there were two sidelines with clonal evolution of one of these sidelines. The basic karyotype had a modal number of 50 chromosomes with trisomy for chromosomes 7, 8, and 12. In addition, an isochromosome for the long arm of chromosome 1, a derived chromosome 2 with a deletion of part of the long arm, and a translocation between the short arm of chromosome 6 and the long arm of chromosome 14 were present. All 21 of the metaphases included in this analysis contained these additional chromosomes and rearrangements. Six metaphases also contained trisomy for chromosome 3. Four of these six had undergone a further rearrangement, having a translocation between the proximal region of the short arm of chromosome 1 and the distal portion of the short arm of chromosome 12. Two other metaphases without the trisomy for chromosome 3 contained a chromosome 1 with the entire long arm deleted. For comparison, the modal chromosome numbers of other prostate lines are PC-3, 58-72 (16); DU 145, 64 (33); ND-1, 62 (25); JCA-1, 69

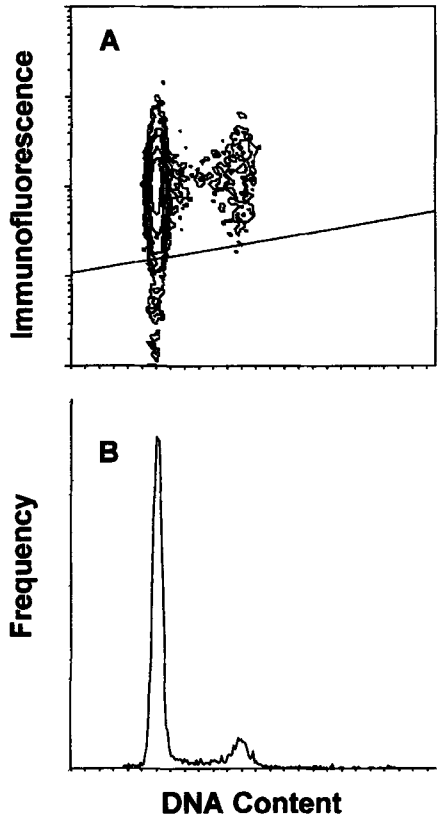

FIG. 3. Flow cytometric analysis of cytokeratin expression and DNA content. *Panel A,* A two-parameter cytogram of 22R*v1* cells stained with anti-CD44 antibody. The diagonal line delineates the level below which events are negative by comparison with a sample stained with an isotype control, nonreactive antibody. *Panel B,* Single parameter histogram of DNA content for the positively stained cells. *Note* low S phase, single stem line, and low level of cells greater than 4C. The *x* axis has 1024 units. *Panels A* and *B, y* axes have a 4 decade and 250 channel range, respectively (arbitrary units).

TABLE 1

DNA-PLOIDY ANALYSIS OF PROSTATE CARCINOMA CELL LINES[a]

	Lymphocytes[b]	LNCaP	DU 145	PC-3	22R*v1* (lp)	22R*v1* (ep)
DNA Index	1.00	2.09	1.60	1.84	1.30	1.40
SD		0.04	0.05	0.06	0.03	0.06

[a]Subconfluent cultures were analyzed by flow cytometry as described in Materials and Methods. N values were 3 or 4 except 22R*v1* (ep) which was 2. lp = late passage; ep = early passage. The difference between 22R*v1* (lp) and 22R*v1* (ep) may be significant ($P > 0.1$; *t*-test with equal variance). LNCaP, DU 145, and PC-3 are prostate carcinoma lines.

[b]Lymphocytes = human blood mononuclear cell preparation.

(22); TSU-Pr1, 80 (14), and DuPro-1, about 96 (8). It may be worth noting that aneusomy of chromosomes 7 and 8 has been associated with prostate cancer (1,5,15,20).

Tumor formation in nude mice. To test whether this line would form tumors, a nude mouse was injected with 1.9×10^7 cells suspended in 0.5 ml Matrigel. Three wk later, a 2.54-g tumor was excised. Serum levels of PSA were 7.0 ng/ml/gram of tumor. Four mice were subsequently injected with cells from this tumor. Tumors formed in all four mice. Part of the tumor was recultured on plastic dishes without feeders, part was subjected to cytogenetic analysis, and part was fixed and embedded in paraffin for histopathological analysis. The cultured tumor displayed significant levels of viable, nonepithelial mouse cells (Fig. 1 *C*). The karyotype of the tumor was identical to that determined for the 22R*v1* line cultured in vitro except that two metaphases were present without trisomy for chromosome 3 and with a chromosome 1 with the entire long arm deleted. As illustrated in Fig. 4, the cell line formed a poorly differentiated carcinoma (Gleason sum 9) with some irregular glands similar to the original relapsed xenograft.

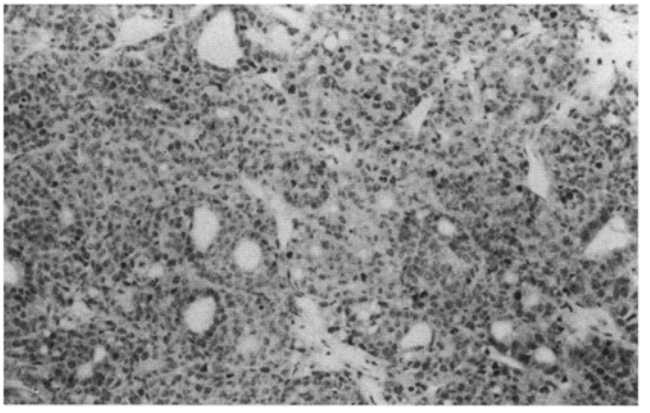

FIG. 4. Representative histopathology of the prostate cancer xenograft that results from injection of 22R*v1* cells into nude mice. The tumors consist of a mixture of poorly differentiated cells that do not form glands (like xenografts of DU 145, PC-3, and LNCaP) and cells that form irregular glandular lumina (hematoxylin and eosin; magnification, ×130).

Population growth phenotype. The cell line 22R*v1* grows slowly to high density. A representative growth curve in 10% serum is shown in Fig. 5 with DU 145 cells for comparison. The doubling time on STO feeders or scraped plates was 49 h (data not shown). The saturation density reached 1.6×10^5 cells/cm^2 at 12 d after plating. On plastic, the doubling time was 35–40 h (Fig. 6). The 22R*v1* saturation density on plastic tissue culture plates was 3×10^5 cells/cm^2 at 16 d after plating. In comparison, DU 145 had a doubling time of 29 h and saturation density of 8.2×10^4 cells/cm^2 achieved between Days 5 and 12 (Fig. 5). Exponential growth was complete by Day 5 for DU 145 when starting at 5×10^5 cells per 10-cm dish. 22R*v1* is like LNCaP in doubling time but different from LNCaP, PC-3, and DU 145 for saturation density (Fig. 6). The colony-forming efficiency of 22R*v1* at low plating density on plastic tissue culture dishes (100–1000 cells per 10-cm dish) was between 10 and 20%.

Androgen receptor expression. The CWR22 xenograft has been shown to express an androgen receptor mRNA and protein, and a point mutation at codon 874 has been identified (35). Since the 22R*v1* cell line is derived from the CWR22R xenograft that was serially transferred after androgen ablation of the androgen-dependent CWR22 xenograft, the response of this line to androgens is of some interest. We asked whether androgen receptor protein was present by immunoblotting immunoprecipitates from 22R*v1* and other prostate cell lines (Fig. 7). LNCaP cells were used as a positive control and PC-3 or DU 145 as potential negative controls. MLC cells had been shown to express androgen receptors (J. S. Rhim,

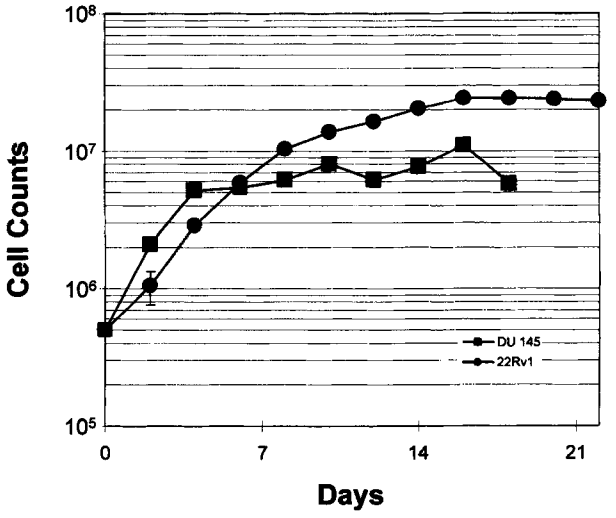

FIG. 5. In vitro growth kinetics of 22R*v1* and DU 145 cell lines. Cells were plated at 5×10^5 per 10-cm dish. The substrates were normal tissue culture plastic for DU 145 cells (squares) and 22R*v1* cells (circles). Medium was RPMI-1640 with 10% serum for 22R*v1* cells and DMEM with 10% serum for DU 145. PC-3 display kinetics similar to those of DU 145, and LNCaP has an initial doubling time like 22R*v1* cells but a saturation density like that of PC-3 and DU 145 ($\sim 1 \times 10^7$ per 10-cm dish). The fluctuations in DU 145 counts during the plateau phase appear to be real, i.e., the cultures appear to be unstable at high density and rounds of cell growth/cell death occur.

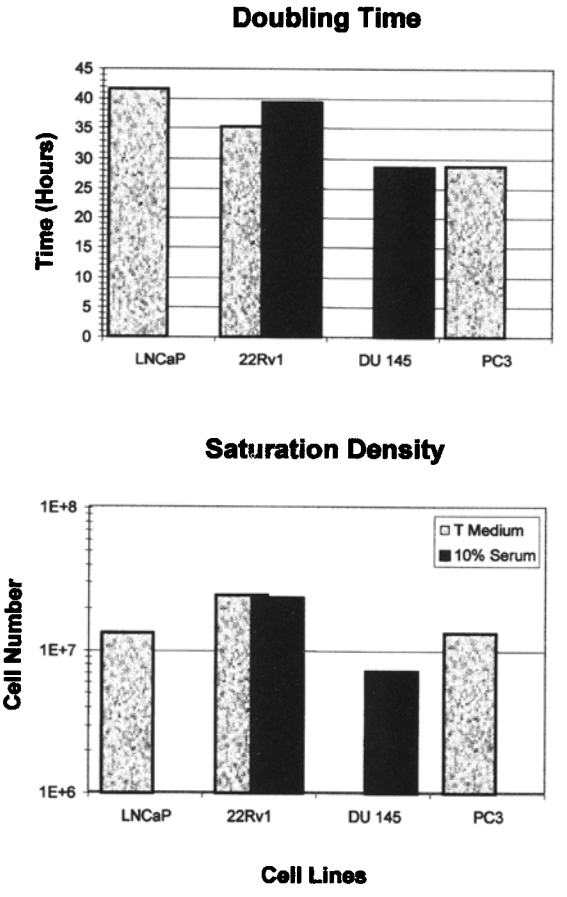

FIG. 6. Growth characteristics of 22R*v1*, LNCaP, DU 145, and PC-3. Cells were plated in either DMEM with 10% serum or T medium (5% serum) and counted as a function of time. Doubling time was calculated from the exponential phase of growth curves and saturation density was calculated from the plateau phase (as in Fig. 3).

unpublished results) and were used as a second positive control. LNCaP are androgen responsive and have been consistently reported to express androgen receptors, whereas DU 145 and PC-3 have been consistently reported to be unresponsive but variously reported to either express (or not) mRNA, protein, or androgen ligand binding (2,6,17,31,34,36). The results (Fig. 7) show a strong band for LNCaP and weaker bands for the other cell lines including MLC and 22R*v1*. The weakest bands were detected in PC-3 and DU 145.

Growth stimulation by Dihydroxytestosterone (DHT), EGF, and TGF-β1. 22R*v1* cells were plated in DMEM without serum or other additives except either DHT, EGF, TGF-β1, or DHT + EGF. Population growth was assayed on Days 3 and 6 by cell counting. The results for Day 6 are presented in Fig. 8. A positive dose response was demonstrated for DHT that was additive with EGF. Significant growth was also detected on Day 3 with DHT, EGF, or DHT + EGF (not shown). There was a small enhancement of cell growth by TGF-β1. This small effect has been measured consistently on average in several experiments; however, since the normal epithelial response to TGF-β1 is growth arrest and cell death, this represents an abnormal response. In work that will be reported in detail elsewhere, we have detected abnormally low expression of the TGF-β type II receptor RNA by reverse transcription-polymerase chain reaction, whereas RNA for the type I receptor, Smad2, and Smad4 are expressed at the same levels as in the TGF-β1-responsive PC-3 and DU 145 cells. The TGF-β-responsive genes $p21^{WAF-1}$ and *PAI-1* were not induced by TGF-β1 treatment. The level of the amplified fragment of type II RNA in 22R*v1* is approximately the same as that of LNCaP cells. LNCaP have been reported to be defective in type II expression and have been reconstituted by transfer of the type II receptor cDNA (11). Therefore, 22R*v1* does not respond normally to

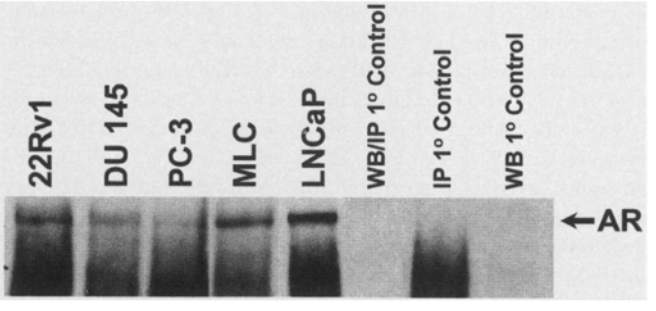

FIG. 7. Androgen receptor (AR) detection. Lysates of each cell line were subjected to immunoprecipitation (IP) with anti-AR polyclonal antibody, electrophoresed, electroblotted and then detected with the same primary antibody and horseradish peroxidase conjugated secondary antibody (WB). Control lanes are IP/WB 1° Control = no primary antibody used in either the IP or WB; IP 1° Control = no primary antibody used in the IP; WB 1° Control = no primary antibody used in the WB. Control samples were LNCaP cells. MLC cells are an immortalized human prostate cell line (3).

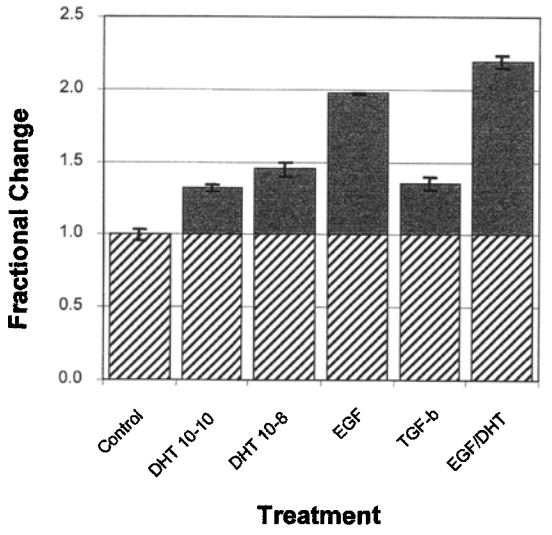

FIG. 8. Hormone and growth factor response. 22R*v1* cells were treated in serum-free medium for 6 d with DHT, EGF, DHT + EGF, or TGF-β1. Changes in cell number relative to the control cells without additives were calculated on triplicate culture plates. Thus, a twofold change in cell number equals 2.0 fractional change whereas 1 represents identity with control cells.

TGF-β1 and the pathway appears to be defective at the level of the type II receptor.

Concluding remarks. Currently, prostate cancer cell lines are few (7), and cell lines derived from primary prostate carcinoma are not widely available (26). DU 145 and PC-3 were derived from brain and bone metastases, respectively (16,21). LNCaP cells were derived from a lymph node metastasis (13). LNCaP-FDG and androgen-resistant variants were derived from in vitro passage of LNCaP cells (26). The scarcity of prostate cancer cell lines compared to the numbers for other solid tumors indicates that lines are difficult to establish from explants of prostate tissue. Serially transplanted xenografts have been more successful (28). In our hands, several attempts to isolate cell lines from the CWR22 and CWR22R xenografts did not succeed due to overgrowth by mouse fibroblasts. To address this, we investigated serial cell sorting and feeder layer enhancement of tumor cell growth to improve the likelihood of cell line derivation. We hope that this approach will help us to derive more prostate carcinoma cell lines. We have tried this same strategy with CWR22 without success. Disassociated cells from the CWR22 xenograft formed colonies on STO feeder layers but eventually were overgrown with mouse cells. So far, we have noted these things about CWR22. The cells appear to have a very low plating efficiency; they form colonies on feeder layers with an initial burst of growth, but growth slows dramatically and does not appear to restart easily by replating on new feeder layers. We have been able to eliminate mouse cells by treatment with cytosine arabinoside (this does not work with CWR22R xenograft cells since they proliferate well and are killed efficiently) but have not succeeded at serial passage. Equally, cell sorting has not worked because the number of colonies that formed after sorting was considerably reduced compared to initial platings. While we do not have enough experience to draw many conclusions from these observations, we can say that in tissue culture (1–10% serum, with or without DHT) the proliferation phenotype of CWR22 is very different from that of CWR22R.

The parent xenograft of 22R*v1* is a relapsed xenograft from castrated mice carrying the androgen-dependent xenograft, CWR22 (23). This xenograft was derived from a primary prostatic carcinoma (Gleason sum 9) from a patient with osseous metastases (28). As a model, CWR22/CWR22R/22R*v1* offers the advantages that 1) the original xenograft was derived from primary human prostate cancer, 2) all express prostate specific antigen, 3) the xenograft model represents primary and relapsed cancer, and 4) we now have a cell line counterpart for in vitro/in vivo experimentation for the relapsed component. As an additional prostate carcinoma cell line, 22R*v1* has a unique genotype and phenotype compared to the widely available DU 145, PC-3, and LNCaP. 22R*v1* has fewer chromosomes and a simpler karyotype with a low degree of variation (15/21 metaphases had 50 chromosomes; 6 metaphases had 51). It is also trisomic for chromosomes 7 and 8 which are common findings in advanced prostate cancers.

It is worth noting, as pointed out by one of the reviewers of this paper, that although hormone-responsive prostate carcinoma cell lines have been isolated and propagated, hormone-dependent cell lines have not. The very different phenotype of CWR22 which is hormone-dependent and CWR22R which is not, and the relative ease with which CWR22R was established as a cell line, suggests that hormone dependency may be more complex than expression and response of the normal or mutated androgen receptor. However, this is speculative—CWR22/CWR22R could be a unique case. Study of CWR22/CWR22R xenografts and the 22R*v1* cell line may lead to hypotheses that could be tested by additional hormone-dependent and independent xenograft pairs or perhaps mouse models.

ACKNOWLEDGMENTS

This work was supported by NCI Cancer Center grant CA 43703 (Athymic Animal, Flow Cytometry, Molecular Cyto-genetics, Radiation, and Tissue Histology Core Facilities), a developmental grant from the CWRU/University Hospitals Cancer Research Center to J. W. J., and CA 57179 to T. G. P.

REFERENCES

1. Barranco, M. A.; Alcaraz, A.; Corral, J. M.; Sole, M.; Mallofre, C.; Llopis, J.; Rodriguez, A.; Ribal, M. J.; Alvarez-Vijande, R.; Carretero, P. Numeric alterations in chromosomes 7 and 8 detected by fluorescent in situ hybridization correlate with high-grade localized prostate cancer. Eur. Urol. 34:419–425; 1998.
2. Brolin, J.; Skoog, L.; Ekman, P. Immunohistochemistry and biochemistry in detection of androgen, progesterone, and estrogen receptors in benign and malignant human prostatic tissue. Prostate 20:281–295; 1992.
3. Chah, J. A.; Rhim, J. S. Current status of prostate cancer research: development of in vitro model systems. Int. J. Oncol. 5:1233–1242; 1994.
4. Cheng, L.; Sun, J.; Pretlow, T. G.; Culp, J.; Yang, N. S. CWR22 xenograft as an ex vivo human tumor model for prostate cancer gene therapy. J. Natl. Cancer Inst. 88:607–611; 1996.
5. Cui, J.; Deubler, D. A.; Rohr, L. R.; Zhu, X. L.; Maxwell, T. M.; Changus, J. E.; Brothman, A. R. Chromosome 7 abnormalities in prostate cancer detected by dual-color fluorescence in situ hybridization. Cancer Genet. Cytogenet. 107:51–60; 1998.
6. Culig, Z.; Klocker, H.; Eberle, J.; Kaspar, F.; Hobisch, A.; Cronauer, M. V.; Bartsch, G. DNA sequence of the androgen receptor in prostatic tumor cell lines and tissue specimens assessed by means of the polymerase chain reaction. Prostate 22:11–22; 1993.
7. Ellis, W. J.; Vessella, R. L.; Buhler, K. R.; Bladou, F.; True, L. D.; Bigler, S. A.; Curtis, D.; Lange, P. H. Characterization of a novel androgen-sensitive, prostate-specific antigen-producing prostatic carcinoma xenograft: LuCaP 23. Clin. Cancer Res. 2:1039–1048; 1996.

8. Gingrich, J. R.; Tucker, J. A.; Walther, P. J.; Day, J. W.; Poulton, S. H.; Webb, K. S. Establishment and characterization of a new human prostatic carcinoma cell line (DuPro-1). J. Urol. 146:915–919; 1991.
9. Gleave, M.; Hsieh, J. T.; Gao, C. A.; von Eschenbach, A. C.; Chung, L. W. Acceleration of human prostate cancer growth in vivo by factors produced by prostate and bone fibroblasts. Cancer Res. 51:3753–3761; 1991.
10. Grasso, A. W.; Wen, D.; Miller, C. M.; Rhim, J. S.; Pretlow, T. G.; Kung, H. J. ErbB kinases and NDF signaling in human prostate cancer cells. Oncogene 15:2705–2716; 1997.
11. Guo, Y.; Kyprianou, N. Overexpression of transforming growth factor (TGF) beta 1 type II receptor restores TGF-beta 1 sensitivity and signaling in human prostate cancer cells. Cell Growth Differ. 9:185–193; 1998.
12. Guo, Y.; Wu, Y.; Shinde, S.; Sy, M. S.; Aruffo, A.; Liu, Y. Identification of a costimulatory molecule rapidly induced by CD40L as CD44H. J. Exp. Med. 184:955–961; 1996.
13. Horoszewicz, J. S.; Leong, S. S.; Kawinski, E.; Karr, J. P.; Rosenthal, H.; Chu, T. M.; Mirand, E. A.; Murphy, G. P. LNCaP model of human prostatic carcinoma. Cancer Res. 43:1809–1818; 1983.
14. Iizumi, T.; Yazaki, T.; Kanoh, S.; Kondo, I.; Koiso, K. Establishment of a new prostatic carcinoma cell line (TSU-Pr1). J. Urol. 137:1304–1306; 1987.
15. Jenkins, R. B.; Qian, J.; Lee, H. K.; Huang, H.; Hirasawa, K.; Bostwick, D. G.; Proffitt, J.; Wilber, K.; Lieber, M. M.; Liu, W., et al. A molecular cytogenetic analysis of 7q31 in prostate cancer. Cancer Res. 58:759–766; 1998.
16. Kaighn, M. E.; Narayan, K. S.; Ohnuki, Y.; Lechner, J. F.; Jones, L. W. Establishment and characterization of a human prostatic carcinoma cell line (PC-3). Invest. Urol. 17:16–23; 1979.
17. Katsuoka, Y.; Hoshino, H.; Shiramizu, M.; Sakabe, K.; Seiki, K. Autoradiographic and cytochemical localization of androgen in human prostatic cancer cell lines. Urology 28:228–231; 1986.
18. Lee, M. S.; Gakovenko, E.; Yun, J. S.; Weijerman, P. C.; Peehl, D. M.; Chen, L. S.; Rhim, J. S. Characterization of adult human prostatic cells immortalized by polybrene-induced DNA transfection with a plasmid containing an origin-defective SV40 genome. Int. J. Oncol. 821–830; 1994.
19. Marengo, S. R.; Resnick, M. I.; Yang, L.; Chung, J. Y. Differential expression of urinary inter-alpha-trypsin inhibitor trimers and dimers in normal compared to active calcium oxalate stone forming men [see comments]. J. Urol. 159:1444–1450; 1998.
20. Matturri, L.; Biondo, B.; Cazzullo, A.; Montanari, E.; Radice, F.; Timossi, R.; Turconi, P.; Lavezzi, A. M. Detection of trisomy 7 with fluorescence in situ hybridization and its correlation with DNA content and proliferating cell nuclear antigen-positivity in prostate cancer. Am. J. Clin. Oncol. 21:253–257; 1998.
21. Mickey, D. D.; Stone, K. R.; Wunderli, H.; Mickey, G. H.; Vollmer, R. T.; Paulson, D. F. Heterotransplantation of a human prostatic adenocarcinoma cell line in nude mice. Cancer Res. 37:4049–4058; 1977.
22. Muraki, J.; Addonizio, J. C.; Choudhury, M. S.; Fischer, J.; Eshghi, M.; Davidian, M. M.; Shapiro, L. R.; Wilmot, P. L.; Nagamatsu, G. R.; Chiao, J. W. Establishment of new human prostatic cancer cell line (JCA-1). Urology 36:79–84; 1990.
23. Nagabhushan, M.; Miller, C. M.; Pretlow, T. P.; Giaconia, J. M.; Edgehouse, N. L.; Schwartz, S.; Kung, H. J.; de Vere White, R. W.; Gumerlock, P. H.; Resnick, M. I., et al. CWR22: the first human prostate cancer xenograft with strongly androgen-dependent and relapsed strains both in vivo and in soft agar. Cancer Research 56:3042–3046; 1996.
24. Nagabhushan, M.; Pretlow, T. G.; Guo, Y. J.; Amini, S. B.; Pretlow, T. P.; Sy, M. S. Altered expression of CD44 in human prostate cancer during progression. Am. J. Clin. Pathol. 106:647–651; 1996.
25. Narayan, P.; Dahiya, R. Establishment and characterization of a human primary prostatic adenocarcinoma cell line (ND-1). J. Urol. 148:1600–1604; 1992.
26. Pousette, A.; Carlstrom, K.; Henriksson, P.; Grande, M.; Stege, R. Use of a hormone-sensitive (LNCaP) and a hormone-resistant (LNCaP-r) cell line in prostate cancer research. Prostate 31:198–203; 1997.
27. Pretlow, T. G.; Delmoro, C. M.; Dilley, G. G.; Spadafora, C. G.; Pretlow, T. P. Transplantation of human prostatic carcinoma into nude mice in Matrigel. Cancer Res. 51:3814–3817; 1991.
28. Pretlow, T. G.; Wolman, S. R.; Micale, M. A.; Pelley, R. J.; Kursh, E. D.; Resnick, M. I.; Bodner, D. R.; Jacobberger, J. W.; Delmoro, C. M.; Giaconia, J. M., et al. Xenografts of primary human prostatic carcinoma. J. Natl. Cancer Inst. 85:394–398; 1993.
29. Schimenti, K. J.; Jacobberger, J. W. Fixation of mammalian cells for flow cytometric evaluation of DNA content and nuclear immunofluorescence. Cytometry 13:48–59; 1992.
30. Seabright, M. A rapid banding technique for human chromosomes. Lancet 2:971–972; 1971.
31. Sica, G.; Fabbroni, L.; Dell'Acqua, G.; Iacopino, F.; Marchetti, P.; Cacciatore, M.; Pavone-Macaluso, M. Natural beta-interferon and androgen receptors in prostatic cancer cells. Urol. Int. 46:159–162; 1991.
32. Stevens, J. W.; Palechek, P. L.; Griebling, T. L.; Midura, R. J.; Rokhlin, O. W.; Cohen, M. B. Expression of CD44 isoforms in human prostate tumor cell lines [see comments]. Prostate 28:153–161; 1996.
33. Stone, K. R.; Mickey, D. D.; Wunderli, H.; Mickey, G. H.; Paulson, D. F. Isolation of a human prostate carcinoma cell line (DU 145). Int. J. Cancer 21:274–281; 1978.
34. Stubbs, A. P.; Lalani, E. N.; Stamp, G. W.; Hurst, H.; Abel, P.; Waxman, J. Second messenger up-regulation of androgen receptor gene transcription is absent in androgen insensitive human prostatic carcinoma cell lines, PC-3 and DU-145. FEBS Lett. 383:237–240; 1996.
35. Tan, J.; Sharief, Y.; Hamil, K. G.; Gregory, C. W.; Zang, D. Y.; Sar, M.; Gumerlock, P. H.; deVere White, R. W.; Pretlow, T. G.; Harris, S. E., et al. Dehydroepiandrosterone activates mutant androgen receptors expressed in the androgen-dependent human prostate cancer xenograft CWR22 and LNCaP cells. Mol. Endocrinol. 11:450–459; 1997.
36. Tilley, W. D.; Wilson, C. M.; Marcelli, M.; McPhaul, M. J. Androgen receptor gene expression in human prostate carcinoma cell lines. Cancer Res. 50:5382–5386; 1990.
37. Wainstein, M. A.; He, F.; Robinson, D.; Kung, H. J.; Schwartz, S.; Giaconia, J. M.; Edgehouse, N. L.; Pretlow, T. P.; Bodner, D. R.; Kursh, E. D., et al. CWR22: androgen-dependent xenograft model derived from a primary human prostatic carcinoma. Cancer Res. 54:6049–6052; 1994.